Comparison of Retinal Waveform between Normal and *rd/rd* Mouse

Jang Hee Ye*, Je Hoon Seo†, Yong Sook Goo*

Departments of *Physiology and †Anatomy, Chungbuk National University School of Medicine, Cheongju, Korea

Retinal prosthesis is regarded as the most feasible method for the blind caused by retinal diseases such as retinitis pigmentosa or age-related macular degeneration. One of the prerequisites for the success of retinal prosthesis is the optimization of the electrical stimuli applied through the prosthesis. Since electrical characteristics of degenerate retina are expected to differ from those of normal retina, we investigated differences of the retinal waveforms in normal and degenerate retina to provide a guideline for the optimization of electrical stimulation for the upcoming prosthesis. After isolation of retina, retinal patch was attached with the ganglion cell side facing the surface of microelectrode arrays (MEA). 8×8 grid layout MEA (electrode diameter: 30 μm, electrode spacing: 200 μm, and impedance: 50 kΩ at 1 kHz) was used to record in-vitro retinal ganglion cell activity. In normal mice (C57BL/6J strain) of postnatal day 28, only short duration (<2 ms) retinal spikes were recorded. In *rd/rd* mice (C3H/HeJ strain), besides normal spikes, waveform with longer duration (~100 ms), the slow wave component was recorded. We attempted to understand the mechanism of this slow wave component in degenerate retina using various synaptic blockers. We suggest that stronger glutamatergic input from bipolar cell to the ganglion cell in *rd/rd* mouse than normal mouse contributes the most to this slow wave component. Out of many degenerative changes, we favor elimination of the inhibitory horizontal input to bipolar cells as a main contributor for a relatively stronger input from bipolar cell to ganglion cell in *rd/rd* mouse.

Key Words: Degenerate retina, Retinal waveform, Multielectrode array, Bipolar cell, Ganglion cell

INTRODUCTION

Photoreceptor loss as a result of retinal degenerative diseases, such as retinitis pigmentosa (RP) and age-related macular degeneration (AMD) are the leading causes of blindness in adults.[1] In retinal degenerative diseases, such as RP and AMD, the majority of cell death occurs in the outer nuclear layer (ONL) containing the photoreceptors (PRs) which transform the light signal to electrical signal.[2,3]

A number of animal models for retinal degeneration have been developed, and the most extensively studied animal is the *rd1* (formerly *rd*, now *Pde6b*^{rd1}) mouse.[4] Mutations in the gene encoding the subunit of cGMP-phosphodiesterase (PDE) have been found in human patients suffering from autosomal recessive RP.[5]

Treatment modalities for the degenerate retina such as gene therapy,[6] and retinal transplantation[7] have shown only limited success. Visual prosthesis is feasible treatment modality which could restore useful vision for the blind. Several groups are actively involved in retinal prosthesis projects.[8,9] Recently a Korean research group focusing on the development of a retinal prosthesis also has been launched.[10]

For retinal prosthesis projects to succeed several prerequisites must be completed. The most important prerequisites is the optimization of electrical stimuli applied through the prosthesis.[9,11] Since the electrical characteristics of diseased retina are expected to differ from those of normal retina, the differences in the electrical characteristics between normal and degenerate retina should be investigated for the optimal stimulation. Therefore, we investigated the differences of electrical characteristics between normal and degenerate retina. Some preliminary results have been presented in Ye *et al.*[12]

This work was supported by the research grant of the Chungbuk National University in 2007.
Submitted May 30, 2008, Accepted September 1, 2008
Corresponding Author: Yong Sook Goo, Department of Physiology, Chungbuk National University School of Medicine, 12, Gaeshin-dong, Hungduk-gu, Cheongju 361-763, Korea.
Tel: 043)261-2870, Fax: 043)272-1603
E-mail: ysgoo@chungbuk.ac.kr

MATERIALS AND METHODS

1. Recording of retinal activity

C57BL/6J strain was used for normal mice and C3H/HeJ strain (*rd/rd* mice) for the retinal degeneration model. The method of Cho *et al*[13] was employed for retinal preparation. Briefly, the eyeball was enucleated and only the retina was isolated. From the isolated mouse retina, a retinal segment (~5×5 mm) was attached with the ganglion cell side on to the surface of multielectrode arrays (MEA). The retinal preparation was carried out under moderate illumination in artificial cerebrospinal fluid (ACSF) solution (solutes in mM: 124 mM NaCl, 10 mM Glucose, 1.15 mM KH_2PO_4, 25 mM $NaHCO_3$, 1.15 mM $MgSO_4$, 2.5 mM $CaCl_2$, and 5 mM KCl) bubbled with 95% O_2, and 5% CO_2 with a pH of 7.3~7.4 at a temperature of 32°C. The composite of high divalent (Hi-Di) solution which blocks the polysynaptic component of postsynaptic potential[14] was 135 mM NaCl, 5.5 mM Glucose, 10 mM HEPES, 15 mM $NaHCO_3$, 5 mM $MgCl_2$, 10 mM $CaCl_2$, and 3.5 mM KCl with a pH of 7.3~7.4. All pharmacological agents were dissolved in oxygenated ACSF solution and were delivered to the retina by continuous superfusion of ACSF at a rate of 1 ml/min. Blocking the ganglion cell spike was achieved with a Na^+-channel blocker, tetrodotoxin (TTX; 0.1 μM). The glutamatergic synapse blocking was achieved by simultaneous treatment with a specific AMPA/kainate receptor blocker, 6-cyano-7-nitroquinoxaline-2, 3-dione (CNQX; 50 μM) and specific NMDA receptor blocker, 2-amino-phosphonoheptanonic acid (AP-7; 100 μM). The glycinergic synapse blocking was in turn achieved with strychnine (100 μM) treatment whereas the GABAergic synapse blocking was achieved with a nonspecific GABA receptor blocker, picrotoxin (100 μM). Specific GABAergic synapse blocking was achived with specific $GABA_A$, $GABA_B$, $GABA_C$ blocker, SR-95531 (100 μM), 2-hydoxysaclofen (100 μM), and 1,2,5,6-tetrahydropyridin-4-yl-methylphosphinic acid (TPMPA; 100 μM), respectively.

2. Electrode and data recording system

The MEA system includes electrode array, stimulator (STG1004, Multi Channel Systems MCS GmbH, Germany), amplifier (MEA1060, Multi Channel Systems GmbH, Germany), temperature control units, and data acquisition hardware and software. The array has 60 active electrodes in an 8×8 layout grid with electrode diameters of 30 μm and inter-electrode distance of 200 μm coated with porous titanium nitride (TiN) to minimize electrical impedance. The impedance level of MEA is 50 kohm at 1 kHz. The amplifier was placed in a Faraday cage with a laboratory-made ground system. Raw data from the MEA was amplified by MEA 1060 amplifiers (amplification: ×1,200, sampling frequency: 25 kHz/channel). Photopic 1.37 μW/cm^2 full field illumination was applied for light stimulation. The light intensity was measured with IL1400A Photometer (International Light Inc, USA). Synchro-

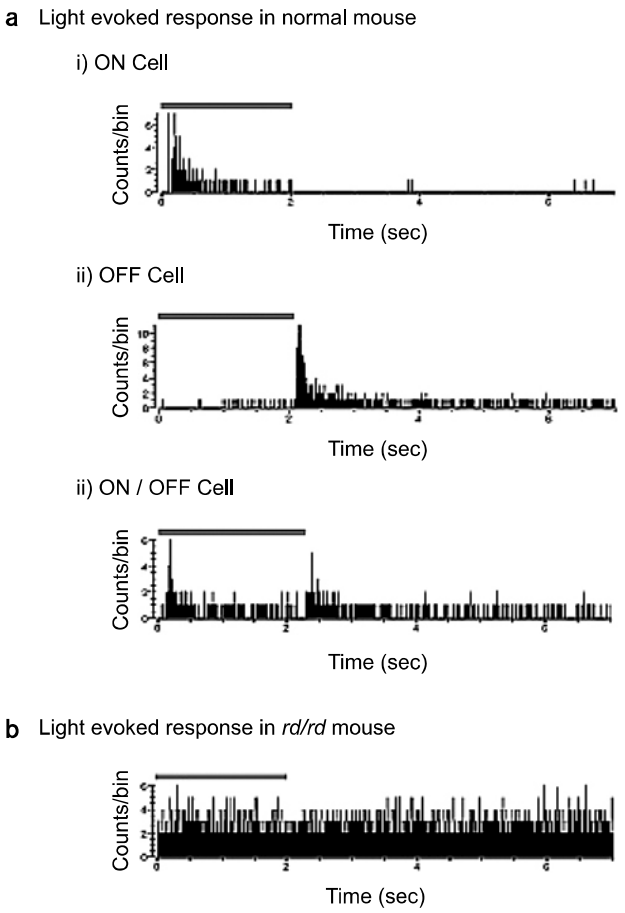

Fig. 1. Light evoked ganglion cell responses classified with PSTH (Post-stimulus time histogram, bin: 1 ms). Gray bars indicate light stimuli (ON: 2 sec, OFF: 5 sec, full field white light illumination of 1.37 μW/cm^2 intensity). (a) Three types of light evoked ganglion cell responses in normal mouse were shown (bin: 1 ms). i) ON cell, ii) OFF cell, and iii) ON/OFF cell. (b) There is no light evoked ganglion cell response in *rd/rd* mouse. All the data were recorded from the retina of normal and the *rd/rd* mice in postnatal day 28.

nization of light stimulus and data recording was accomplished through RS232C output port.

RESULTS

1. No light evoked response in *rd/rd* mice (Fig. 1)

After postnatal day (PD) 14, retinal ganglion cell responses were categorized as ON, OFF and ON/OFF in normal mice with light stimulation. But in the *rd/rd* mice, there was no light evoked response as expected. The light evoked responses were recorded with PD28 normal mice (n=3) and *rd/rd* mice (n=7). Each representative ON, OFF, and ON/OFF cell in normal mouse were shown (Fig. 1a). And one exemplar PSTH with light stimulation in *rd/rd* mice was shown (Fig. 1b).

2. Histological findings and retinal recordings with MEA (Fig. 2)

Whole mount sections of retina were stained with cresyl violet in the normal mice and *rd/rd* mice. From neonate to PD7, no differences between normal and *rd/rd* mice were found both in retinal histology and retinal waveforms. But from PD14, remarkable differences both in histology and retinal recording were observed in *rd/rd* mice. While outer nuclear layer (ONL) and outer plexiform layer (OPL) developed from neuroepithelium in normal mice, no ONL and OPL were found in *rd/rd* mice. And the retinal waveform recording showed rather complex shapes in the *rd/rd* mice. After PD14, besides spike, additional slow wave component of approx-

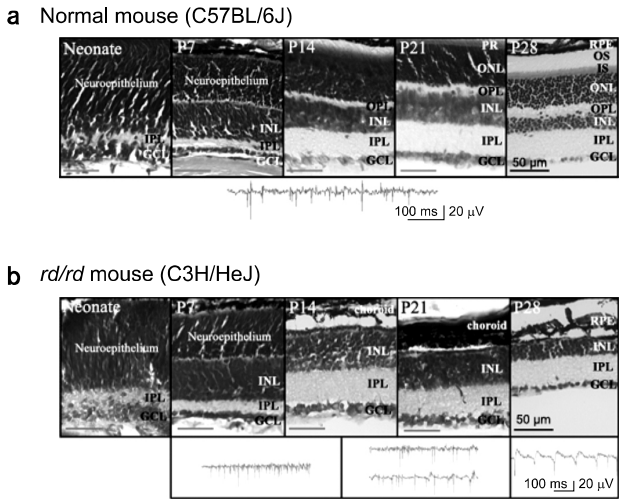

Fig. 2. Retinal histology and retinal recording in normal and *rd/rd* mouse. Top: Retinal histology from neonate, postnatal day (PD) 7, PD14, PD21, and PD28 mouse. Retinal tissues were whole mount sectioned and stained with cresyl violet. RPE, retinal pigment epithelium; PR, photoreceptor; OS, IS, outer and inner segments of photoreceptor; ONL, outer nuclear layer; OPL, outer plexiform layer; INL, inner nuclear layer; IPL, inner plexiform layer; GCL, ganglion cell layer. Scale bar, 50 um. Bottom: Retinal waveform recording with MEA.

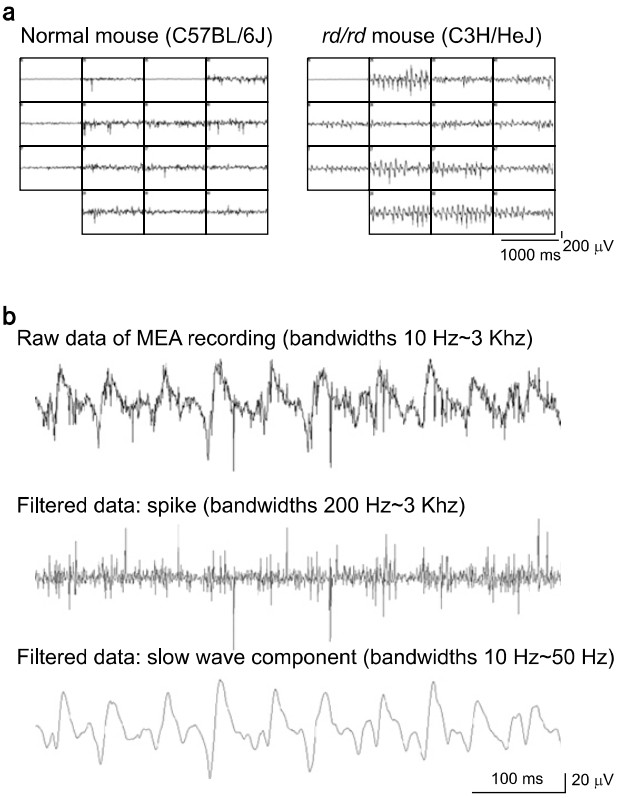

Fig. 3. Isolation of fast spike and slow wave component. (a) Lower left quadrant of display window of data acquisition software (MC_Rack) which shows 60 channels of an 8×8 multi-electrode array. The recording was acquired from *in vitro* retinal preparation of normal and *rd/rd* mice in PD28. The channel number is shown on the upper left part of each channel (e.g. Channel 25 means the channel of 2nd column and 5th row). Channel 15 is the internal ground. (b) Isolation of spike and slow wave component from the retinal recording in *rd/rd* mice. Top trace: MEA recording with a bandwidth of 10 to 3,000 Hz from channel 25 of Fig. 3a which shows a combination of fast spikes and slow wave component. Middle trace: Isolation of spikes from top trace using a high pass filter with a 200 Hz cut-off frequency. The bandwidth ranges from 200 to 3,000 Hz. Bottom trace: Isolation of the slow wave component from top trace using a low pass filter with a 50 Hz cut-off frequency. The bandwidth ranges from 10 to 50 Hz.

imately 100 ms duration appeared in some parts of retina, while only spikes of short duration (<2 ms) were present in other parts of retina in *rd/rd* mice. With aging, the slow wave component became dominant, so that after PD28 the slow wave component was present in entire retina of the *rd/rd* mice. On PD14, the slow wave component appeared in a few channels (7 of 116 channels, retinal preparation number, n=2). The percentage of the slow wave component-positive channel was 20.30±0.04% (n=4) on PD21 and it significantly increased to 37.90±0.07% (n=6) on PD28 ($p<0.01$). However, in normal mice the slow wave component did not appear regardless of age up to PD42 (PD14; n=2, PD21; n=2, PD28; n=6, PD35; n=3, PD42; n=2).

3. Isolation of fast spike and slow wave component from retinal waveform recordings with MEA (Fig. 3)

Fig. 3a depicts typical recordings of spontaneous retinal activity from PD28 normal and *rd/rd* mouse by MEA (lower left quadrant of displayed window on the computer monitor with the Mc_Rack software). In most electrode channels, both spikes and the slow wave component were observed in *rd/rd* mouse. Since most electrode channels show both spikes and the slow wave component, the data were filtered to isolate each component. From the MEA recording with a bandwidth ranging from 10 to 3,000 Hz, a high pass filter with a cut-off frequency of 200 Hz and a low pass filter with a cut-off frequency of 50 Hz were applied to isolate spikes and the slow wave component, respectively (Fig. 3b).

4. Effects of synaptic blockers on slow wave component (Fig. 4)

To investigate the mechanism of the slow wave component, various synaptic blockers were applied so they would react at different synapses.[15] Since 100 ms-long duration slow wave component in comparison with very short spikes of (<2 ms) suggest that it may not be originate in the ganglion cell origin but rather is mediated through retinal synapses. We tested this possibility using Hi-Di solution and TTX (Fig. 4a, b). The Na^+-channel blocker, TTX (n=3), reveals that only the slow wave component remains, while spikes are blocked, which strongly supports the idea that the slow wave component does not originate in the ganglion cell. With the Hi-Di solution

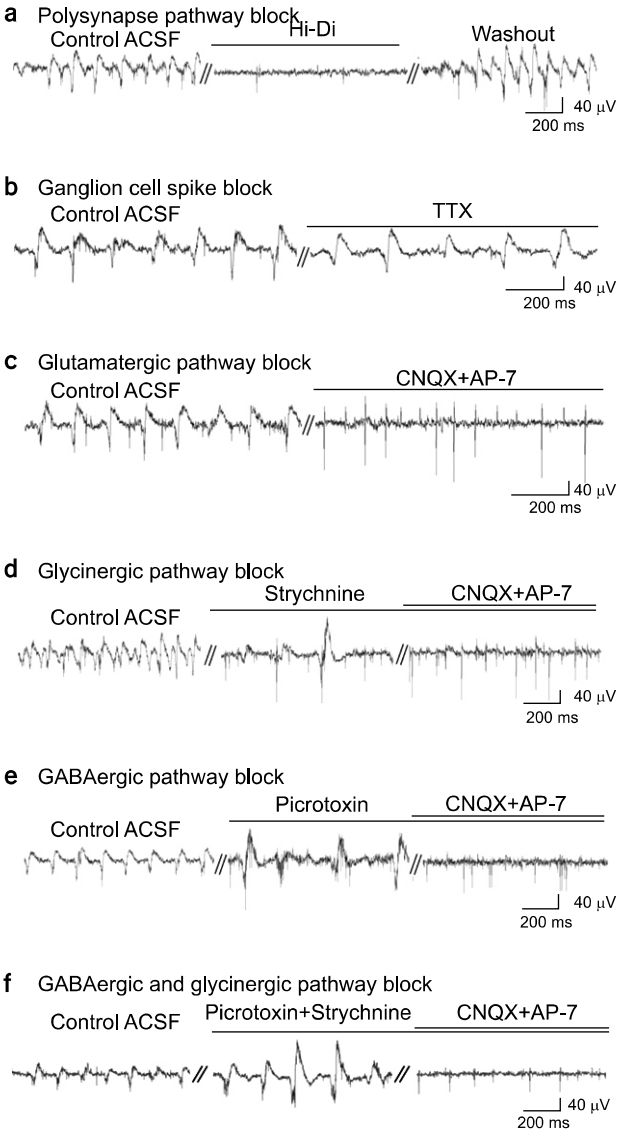

Fig. 4. Effects of various blockers. (a) Treatment of Hi-Di ACSF solution completely blocked the slow wave component (n=4). Effect of Hi-Di was reversible. (b) TTX blocked spikes however, slow wave components remained (n=3). (c) Effect of glutamatergic synapse blocking. When treated with both CNQX and AP-7 simultaneously, the slow wave component disappeared however, fast spikes still remained. (d) Effect of glycinergic synapse blocking. When treated with strychnine, the amplitude of the slow wave component increased. (e) The effect of GABAergic synapse blocking. The picrotoxin effect on the amplitude of the slow wave component was similar to the strychnine effect. (f) The effect of glutamatergic, glycinergic, and GABAergic synapse blocking. With picrotoxin and strychnine, the amplitude of slow wave component increased. With the additional treatment of CNQX/AP-7 in (d), (e), and (f), only fast spikes remained. All the data were acquired from different retinal preparations of PD28 *rd/rd* mice. All the recordings shown were at 5 minutes after application of control ACSF or each blocker.

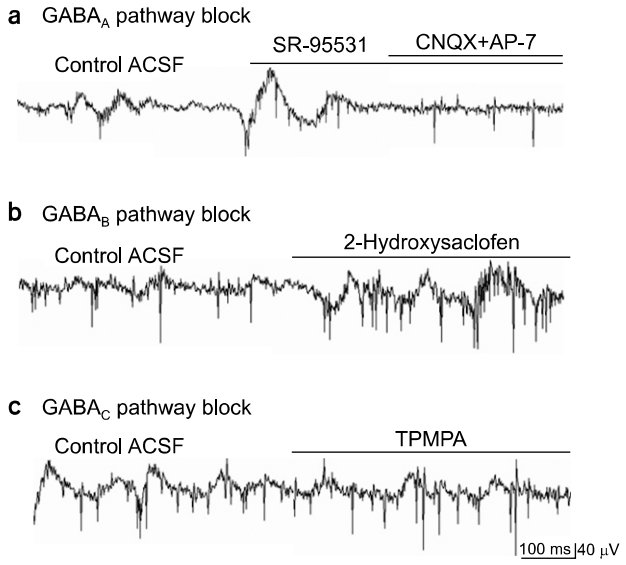

Fig. 5. Effects of specific GABAergic synapse blocking. (a) When treated with specific $GABA_A$ blocker, SR-95531, the amplitude of the slow wave component increased. (b) When treated with specific $GABA_B$ blocker, 2-Hydroxysaclofen, no significant change of the slow wave component occurred. (c) When treated with specific $GABA_C$ blocker, TPMPA, no significant change of the slow wave component occurred.

(n=4), which blocks excitatory postsynaptic potential (EPSP), the slow wave component was completely blocked. Therefore, we confirmed that the slow wave component is mediated through retinal synapses.

To investigate the detailed mechanism of the slow wave component, we applied various synaptic blockers to affect different synapses.[15] First, glutamate antagonists were applied. Since the glutamatergic pathway is a major excitatory synapse for the retina, specific AMPA/kainate receptor blockers, CNQX and AP-7 were applied together. With this co-treatment, the slow wave component were blocked while the less dominant retinal spikes became more apparent. (n=7) (Fig. 4c). Second, the effects of strychnine (n=7) was tested (Fig. 4d), since the glycinergic pathway is one of the major inhibitory synapses of the retina. The amplitude was 58.8±17.7 μV without strychnine while it significantly increased to 152.8±73.5 μV with strychnine (retinal preparation number, n=3, channel number, n=25, $p<0.001$). With the additional treatment of CNQX/AP-7, the slow wave component was blocked while the fast spikes remained, which was similar to the observations with CNQX/AP-7 applied. Third, the GABAergic antagonist, picrotoxin was applied (Fig. 4e), since the GABAergic pathway is another important inhibitory synapse of the retina. The amplitude of the slow wave component increased from 41.2±14.5 to 83.7±19.6 μV with picrotoxin (retinal preparation number, n=3, channel number, n=28, $p<0.001$). Fourth, specific GABAnergic antagonists were applied. The effect of GABAA blocker, SR-95531 (n=3) appeared to be similar with that of strychnine and picrotoxin, while neither GABAB blocker, 2-hydroxysaclofen (n=3) nor GABAC blocker, TPMPA (n=3) made any significant effects on retinal waveforms (Fig. 5).

DISCUSSION

1. 100 ms-long duration slow wave component in retina

The slow wave component (~100 msec) has not been reported previously in *rd/rd* mouse retina. Most retinal recordings with MEA are filtered to obtain a bandwidth ranging from 20 to 2,000 Hz to sort either fast RGC spikes[16,17] or a bandwidth ranging from 0.5 to 100 Hz to sort slow wave component-like microERG18) for a different research purpose. Because our research goal was to compare electrical characteristics of retina between normal and *rd/rd* mouse, data with a bandwidth of 10 to 3,000 Hz were obtained. In the *rd/rd* mice, the slow wave component was observed in addition to fast spikes while only fast spikes were observed in normal mouse. Each component was isolated with different filter setting (Fig. 3).

2. The underlying mechanism of slow wave component

Our results show that the slow wave component of *rd/rd* mice is not the spike of ganglion cell but the EPSP through the retinal synapses (Fig. 4). The vertical information processing from photoreceptors through bipolar cells and ganglion cells is modified by lateral interactions with the horizontal and amacrine cells.[19] Since glycine and GABA are the neurotransmitters mediating connections from horizontal and amacrine cells, we tested the effects of the glycinergic antagonist, strychnine and the GABAergic antagonist, picrotoxin. With strychnine and picrotoxin, the enhancement of the amplitude of slow wave component could be explained by the blocking of the inhibitory synapse to the ganglion cells. And with specific GABA blocker study, it was confirmed that the major contrib-

utor for GABA pathway is mediated through GABAA pathway (Fig. 5).

Since the strychnine induced amplitude enhancement of the slow wave component was blocked by CNQX/AP-7, the effect of CNQX/AP-7 should be down-stream of amacrine input to bipolar cell. With the blocking of the glutamatergic synapse, the slow wave component disappeared, suggesting that probably stronger glutamatergic input from bipolar cell to ganglion cell in *rd/rd* mice than normal mice contributes most to this slow wave component. Out of many degenerative changes, we favor elimination of inhibitory horizontal input to bipolar cells resulting from loss of synaptic inhibition, decrease in number of horizontal cells[20,21] in *rd/rd* mice as a main contributor for a relatively stronger input from bipolar cell to ganglion cell in *rd/rd* mice.

CONCLUSION

1. In *rd/rd* mice, besides normal spikes, the slow wave component was recorded.
2. The slow wave component is not the action potential of ganglion cell origin but the EPSP through retinal synapses.
3. We suggest that stronger excitatory glutamatergic input from bipolar cell to the ganglion cell in *rd/rd* mouse than normal mouse contributes the most to the generation of the slow wave component.

REFERENCES

1. **Hyman L**: Epidemiology of eye disease in the elderly. Eye 1(Pt 2):330-341 (1987)
2. **Humayun MS, Prince M, de Juan Jr E, et al**: Morphometric analysis of the extramacular retina from postmortem eyes with retinitis pigmentosa. Investigative Ophthalmology & Visual Science 40:143-148 (1999)
3. **Medeiros NE, Curcio CA**: Preservation of ganglion cell layer neurons in age-related macular degeneration. Investigative Ophthalmology & Visual Science 42:795-803 (2001)
4. **Farber DB, Flannery JG, Bowes-Rickman C**: The rd mouse story: seventy years of research on an animal model of inherited retinal degeneration. Prog Ret Eye Res 13:31-64 (1994)
5. **MacLaren RE, Pearson RA, MacNeil A, et al**: Retinal repair by transplantation of photoreceptor precursors. Nature 444: 203-207 (2006)
6. **Acland GM, Aguirre GD, Ray J, et al**: Gene therapy restores vision in a canine model of childhood blindness. Nature Genetics 28:92-95 (2001)
7. **del Cerro M, Gash DM, Rao GN, et al**: Retinal transplants into the anterior chamber of the rat eye. Neuroscience 21:707-723 (1987)
8. **Zrenner E**: Will retinal implants restore vision? Science 295: 1022-1025 (2002)
9. **Margalit E, Maia M, Weiland JD, et al**: Retinal prosthesis for the blind. Surv Opthalmol 47:335-336 (2002)
10. **Seo J, Zhou J, Kim E, et al**: A retinal implant system based on flexible polymer microelectrode array for electrical stimulation. Tombran-Tink J, Barnstable C, Rizzo JF: *Ophthalmology Research: Visual Prosthesis and Ophthalmic Devices.* New Hope in Sight. Humana Press, New Jerse (2007), pp. 107-119
11. **Lowenstein JI, Montezuma SR, Rizzo III JF**: Outer retinal degeneration: An electronic retinal prosthesis as a treatment strategy. Archives of Ophthalmology 122:588-596 (2004)
12. **Ye JH, Seo JH, Goo YS**: Abnormal retinal waveforms in rd/rd mouse recorded with multielectrode array. World Congress on Biomedical Engineering, Seoul, 3397-3400 (2006)
13. **Cho HS, Jin GH, Goo YS**: Characterization of rabbit retinal ganglion cells with multichannel recording. Korean J Med Physics 15:228-236 (2004)
14. **Liao X, Walters ET**: The use ofelevated divalent cation solutions to isolate monosynaptic components of sensorimotor connections in Aplysia. J Neuroscience Methods 120:45-54 (2002)
15. **Soucy E, Wang Y, Nirenberg S, et al**: Novel signaling pathway from rod photoreceptors to ganglion cells in mammalian retina. Neuron 21:481-493 (1998)
16. **Meister M, Pine J, Baylor DA**: Multi-neuronal signals from the retina: acquisition and analysis. J Neuroscience Methods 51:95-106 (1994)
17. **Devries SH**: Correlated firing in rabbit retinal ganglion cells. Journal of Neurophysiology 81:908-920 (1999)
18. **Guenther E, Herrmann T, Stett A**: The retina sensor: An in vitro tool to study drug effects on retinal signaling. Taketani M, Baudry M: *Advances in Network Electrophysiology Using Multi-electrode Arrays.* Springer, New York (2006), pp. 321-331
19. **Dowling JE**: The retina: an Approachable Part of the Brain, Cambridge, MA: Harvard University Press, (1987)
20. **Strettoi E, Pignatelli V**: Modifications of retinal neurons in a mouse model of retinitis pigmentosa. Proc Natl Acad Sci USA 97:11020-11025 (2000)
21. **Strettoi E, Porciatti V, Falsini B, et al**: Morphological and functional abnormalities in the inner retina of the rd/rd mouse. J Neurosci 22:5492-5504 (2002)

정상 마우스와 *rd/rd* 마우스의 망막파형 비교

충북대학교 의과대학 *생리학교실, †해부학교실

예장희*・서제훈†・구용숙*

망막색소변성(retinitis pigmentosa: RP)과 연령관련 황반변성(age-related macular Degeneration: AMD)은 망막변성으로 인해 실명에 이르는 대표적인 질환이며 망막이식장치의 개발을 통해 치료될 수 있다고 간주되고 있다. 성공적인 망막이식장치 개발을 위하여 여러 가지 선결요소가 필요하지만 그 중 한 가지가 이식장치에 인가할 전기자극을 최적화하는 것이다. 변성망막의 전기적 특성은 정상 망막과 다르리라 예측되므로 우리는 장차 개발될 망막 이식장치에 인가할 전기자극 최적화를 위한 가이드라인을 제공하기 위해 정상 망막과 변성망막의 망막파형 차이에 관한 연구를 하였다. 망막을 분리한 후 망막절편을 신경절세포 층이 다채널전극의 표면을 향하게 하여 전극에 붙인다. *In-vitro* 상태에서 망막 신경절세포의 전기신호를 기록하기 위해 전극 직경: 30 μm, 전극간 거리: 200 μm , 전극 임피던스 1 kHz에서 50 kΩ인 8행 8열의 다채널전극을 사용하였다. 생후 28일된 정상마우스(C57BL/6J 종)에서는 짧은 시간대(<2 ms)의 망막 스파이크만 기록되었다. *rd/rd* 마우스(C3H/HeJ 종)에서는 정상적인 스파이크뿐만 아니라 약 100 ms 의 시간대를 가지는 느린 파형이 같이 기록되었다. 우리는 rd/rd 마우스에서만 관찰되는 이 느린 파형의 기전을 알아보고자 여러 가지 시냅스억제제를 사용하였다. 이 느린 파형은 *rd/rd* 마우스에서 양극세포로부터 신경절세포로 들어오는 흥분성입력이 정상마우스보다 강화되었기 때문에 발생한 것으로 보인다. *rd/rd* 마우스에서 흥분성입력이 강화되는 여러 가능성 중에서 망막변성으로 인해 수평세포로부터 양극세포로 들어오는 억제성 입력이 소실됨으로 인해 결과적으로 양극세포로부터 신경절세포로 들어오는 흥분성입력이 강화되었을 가능성이 가장 높은 것으로 보인다.

중심단어: 변성망막, 망막파형, 다채널전극, 양극세포, 신경절세포